

1 **The secret of VDAC isoforms is in their gene regulation? Characterization of**
2 **human VDAC genes expression profile, promoter activity, and transcriptional**
3 **regulators.**

4

5 **Federica Zinghirino¹, Xena Giada Pappalardo¹, Angela Messina^{2,3}, Francesca Guarino^{1,3*}, Vito**
6 **De Pinto^{1,3}**

7

8 ¹ Department of Biomedical and Biotechnological Sciences, University of Catania, Via S. Sofia 64,
9 95123 Catania, Italy.

10 ² Department of Biological, Geological and Environmental Sciences, Section of Molecular Biology,
11 University of Catania, Viale A. Doria 6, 95125 Catania, Italy.

12 ³ National Institute for Biostructures and Biosystems, Section of Catania, Rome, Italy.

13

14

15 *Correspondence:

16 Francesca Guarino, francesca.guarino@unict.it, +390957384231

17

18

19

20 **Abstract**

21

22 **Background:** VDACs (Voltage-Dependent Anion-selective Channels) are pore-forming proteins of
23 the outer mitochondrial membrane, whose permeability is primarily due to their presence. In higher
24 eukaryotes three isoforms raised during the evolution: they have the same exon-intron organization
25 and the proteins show the same channel-forming activity. We provide a comprehensive analysis of
26 the three human VDAC genes (VDAC1–3), their expression profiles, promoter activity, and potential
27 transcriptional regulators.

28 **Results:** VDAC isoforms are broadly but also specifically expressed in various human tissues at
29 different levels with a predominance of VDAC1 and VDAC2 over VDAC3. However, RNA-seq
30 CAGE approach revealed a higher level of transcription activation of VDAC3 gene. We
31 experimentally confirmed this information by reporter assay of VDACs promoter activity.
32 Transcription Factor Binding Sites (TFBSs) distribution in the promoters was investigated. The main
33 regulators common to the three VDAC genes were identified as E2FF, NRF1, KLFS, EBOX
34 transcription factors family members. All of them are involved in cell cycle and growth, proliferation,
35 differentiation, apoptosis, and metabolism. More transcription factors specific for each isoform gene
36 were identified, supporting the results in the literature, indicating a general role of VDAC1, as actor
37 of apoptosis for VDAC2, and the involvement in sex determination and development of VDAC3.

38 **Conclusions:** For the first time, we propose a comparative analysis of human VDAC promoters to
39 investigate their specific biological functions. Bioinformatics and experimental results confirm the
40 essential role of VDAC protein family in mitochondrial functionality. Moreover, insights about a
41 specialized function and different regulation mechanisms arise for the three isoforms genes.

42

43

44 **Keywords:** VDAC isoforms, gene structure, expression profile, core promoter, transcription factors
45 binding sites, mitochondrial function

46 **Background**

47

48 VDAC (Voltage-Dependent Anion-selective Channel) is the prototype of the family of subcellular
49 pores responsible for the permeability of mitochondrial outer membrane [1]. This protein is a key
50 control point for the passage of ions and metabolites to guarantee cell energy production. During
51 evolution more isoforms raised in the eukaryotic organisms [2]: they were characterized by the
52 functional point of view, revealing very close permeability features [3-7]. Also, experiments aimed
53 to study their expression patterns in different tissues indicated very subtle differences and a quite
54 ubiquitous presence in the tested tissues [8].

55 In general, the distribution of VDAC isoforms is more or less ubiquitous in tissues but with a
56 prevalence of VDAC1 isoform. Although the three VDAC genes codify proteins with apparently the
57 same function, differences in the amino acid content, in the localization in the mitochondrial outer
58 membrane layer [9], in the channel functionality and voltage dependence [6, 7], in the contribution
59 of N-terminal portion to cell viability and survival [10], lead to hypothesize a more specialized
60 role/function for each isoform in different biological contexts.

61 Results from various groups highlighted specific functions for each isoform, and it is considered a
62 common notion that, for example, VDAC1 is a pro-apoptotic actor [11], while VDAC2 is an anti-
63 apoptotic protein [12]. The role of VDAC3 was associated with sex tissue development and
64 maintenance soon after its discovery [13, 14]. A further step was the deletion of single isoforms'
65 genes, which was performed in transgenic mice. In VDACs knock-out mice, physiological defects
66 are linked to altered structure and functionality of mitochondria [11, 13]. Mitochondria lacking
67 VDAC (VDAC1-/-), are characterized by increased size, irregular and compacted cristae, and altered
68 respiratory complex activity particularly in various types of muscles [11]. Other alterations have been
69 detected in specific tissue injuries or pathologies like Alzheimer's disease [15, 16]. These
70 abnormalities may concur to produce not functional cells. The absence of VDAC1 in muscle biopsies
71 of child patients with impaired oxidative phosphorylation, suffering for mitochondrial

72 encephalomyopathy, was associated with a fatal outcome [17, 18]. VDAC2^{-/-} knock-out mice could
73 not develop to adult individuals, but only ES cells could be grown [19]. A significant degree of growth
74 retardation characterizes VDAC1/3^{-/-} mice; and VDAC3^{-/-} deficient male mice show the peculiarity
75 to be infertile, with a disassembled sperm tail, the flagellum essential for sperm motility [13]. More
76 recently the amino acid composition of the three mammalian VDAC isoforms was examined,
77 showing interesting peculiarities [20]. The cysteine content of the three isoforms is different and this
78 was correlated to their oxidation and potential disulfide bonds formation [21]. The three isoforms
79 carry strikingly different amounts of cysteine whose different role has been hypothesized [20].
80 Similarly to VDACs knock-out mice, defects in the brain, muscle, and germinal tissues function were
81 observed in *Drosophila melanogaster* porin1 mutants [22]. In the yeast *S. cerevisiae*, two *porin* genes
82 were found but only *porin1* coding VDAC1 is essential for life [23].
83 A peculiar expression of VDAC isoforms was observed in cells and tissue of the germinal lines of
84 different organisms. While VDAC1 is mainly located in cells of reproductive organs necessary to
85 support the development of gametes [24, 25], VDAC2 and VDAC3 are expressed in a specific portion
86 of sperm and oocyte and genetic variants or the aberrant regulation of these genes are correlated with
87 infertility [26, 27].
88 Mechanisms of VDAC genes expression regulation have never been explored in a comparative and
89 systematic way. Only one paper was published, describing the organization and activity of mouse
90 VDAC gene promoters [28]. A prediction of the regulatory regions of the three VDAC isoforms show
91 that the promoters lack the canonical TATA-box and are G+C-rich, the Transcription Start Site (TSS)
92 was identified and the mouse putative VDAC promoters tested for their activity. In more recent years
93 other few reports have been published on VDACs' promoter regulation for specific germinal lineage.
94 The activity of VDAC2 promoter in mammals developing ovary triggered by GATA1 and MYBL2
95 transcription factors lead to autophagy inhibition confirming its relevant role in cell survival [29]. In
96 human male abnormal hypermethylation of VDAC2 promoter correlated with idiopathic
97 asthenospermia while in complete unmethylation or mild hypermethylation, sperm motility improved

98 confirming the role of VDAC2 expression in human spermatozoa [30]. The increased expression
99 level of VDAC1 transcript was also induced by a lncRNA through enhancement of H3K4me3 levels
100 in its promoter leading to apoptosis of placental trophoblast cells during early recurrent miscarriage
101 [31]. For the first time, we propose with this work a study of the genomic region located upstream
102 the TSS generating the three VDACs mRNA. We collected the information on human VDACs genes
103 structures and transcription from the main available public resources. Once VDAC gene promoters
104 were identified, we analyzed the sequences using bioinformatics software to identify Transcription
105 Factors Binding Sites (TFBSs) distribution. We performed experimental tests with a molecular
106 biology approach to confirm the insights obtained and to assess the transcriptional activity. We
107 believe that understanding the molecular mechanisms triggering VDAC genes transcription in
108 physiological and altered conditions might highlight the biological role of each isoforms inside the
109 cells and in different biological contexts.

110

111

112

113 **Results**

114

115 **Structure of human VDAC1, VDAC2 and, VDAC3 genes: transcripts variants and promoters.**

116 The vast amount of large-scale genomic projects, high-throughput sequencing, and transcriptomic
117 data, as well as the plentiful supply of promoter resources, assist in the comprehensive reconstruction
118 of a transcriptional regulatory region. To intersect these data enabled us to provide a framework of
119 the main functional DNA elements for the identification of biochemical active regions supposed as
120 gene promoter sequences of each VDAC isoforms, and to study the transcriptional control of the
121 promoter structure by the analysis of TF-binding sites specificity and co-association patterns with
122 other TFs.

123 Here, we will show the results of merging these clues with information from gene expression profile
124 datasets, and with analysis of the promoter-specific activity of VDACS, which helped to investigate
125 the co-expression relationship and the context-dependent regulation of VDAC genes.

126 Our approach narrowed down the analysis of the promoter region of each VDAC isoform to defined
127 600bp segment for P_{VDAC1} (chr5:133,340,230-133,340,830; hg19) P_{VDAC2} (chr10:76,970,184-
128 76,970,784; hg19) and P_{VDAC3} (chr8:42,248,998-42,249,598; hg19), whose range is from -400 bp to
129 +200 bp relative to TSS of annotated promoter sequences in EPD new (v.006). The boxed area in
130 Figure 1 a-c highlights the UCSC-based BLAT result of P_{VDAC1} , P_{VDAC2} and P_{VDAC3} matching with
131 functional elements positioned within the region of accessible chromatin that define the nearest active
132 promoter sequence. The structural organization of VDACS genes, transcripts, and the surrounding
133 regions were analyzed here.

134 The transcripts coding the three VDACS functional proteins are reported with the code
135 ENST00000265333.8 for VDAC1, ENST00000543351.5 for VDAC2, ENST0000022615.9 for
136 VDAC3 corresponding respectively to NM_003374.2, NM_001324088.1 and NM_005662.7 in the
137 Refseq database of NCBI.

138 Several transcript variants from Ensemble database are also indicated for each VDAC isoforms. Most
139 of the splice variants have the same exons composition compared to the coding transcript but differ
140 in the length of the 5' and 3'. Some of them are processed transcripts, other features retained intron
141 and for VDAC3 two are involved in nonsense-mediated decay mechanism. It is not known whether
142 the other splice variants identified have any functional biological role, however, gene expression data
143 collected from NIH Genotype-Tissue Expression project (GTEx), report the expression of them,
144 including the non-protein coding transcripts.

145 The 600bp-selected promoter region shows a high degree of overlap with the identification of the
146 CpG island and the RNA polymerase II binding site close to the TSS, also confirmed by ChIP-seq
147 data of chromatin-state model and the enrichment levels of the H3K4me1 and H3K4me3 histone
148 marks, chosen as the best predictors of transcription and open chromatin elements available among
149 the UCSC regulation tracks.

150

151 **VDAC genes transcription by Gene Expression Atlas resources**

152 Gene expression profile was highlighted through the analysis of available high-throughput data,
153 included in international collaborative projects aimed to characterize human genome expression and
154 regulation. In this work data, revised and curated by Gene Expression Atlas of EMBL-EBI, from
155 GTEx [32] and RIKEN Functional ANnotation of the Mammalian Genome 5 (FANTOM) project
156 [33], were reported for an interesting comparison of results obtained with RNA-seq methodology.
157 The expression patterns of the three VDAC isoforms depict the level of VDAC transcripts distribution
158 in different human tissues.

159 The RNA-Seq expression data from GTEx, obtained by human tissues samples from post-mortem
160 individuals, show that the level of VDACs mRNA expression seems comparable among the three
161 isoforms but with a prevalence of VDAC1 (Fig. 2 a-b). A relevant result is that all VDAC isoforms
162 are mainly expressed in skeletal muscle and heart comparing the expression with the other tissues.
163 VDAC1 and VDAC3 isoforms are expressed with a similar score while VDAC2 is expressed to a

164 minor extent. Among the other tissues, we noticed that both VDAC1 and VDAC3 are represented in
165 different portions of the brain with a higher score than VDAC2. However, the presence of VDAC1
166 and VDAC3 in brain regions seems to be differentiated since the former isoform is more expressed
167 in diencephalon while VDAC3 in the telencephalon. A similar situation can be observed in organs
168 forming the digestive apparatus. The specificity of VDAC isoforms expression can be highlighted in
169 other tissues. For example, VDAC1 is revealed in skin tissues, exposed or not to sun, kidney, VDAC2
170 in the bladder, cervix/ectocervix, vagina, and VDAC3 in testis.

171 RNA-seq CAGE VDAC transcripts expression were selected from RIKEN FANTOM 5 project. The
172 enrichment of mRNA obtained by this technique is well known to provide the map of TSS and the
173 activity of genes promoter. In Figure 3 the first relevant result, emerging from this analysis, is the
174 higher expression level of VDAC3 transcripts compared to VDAC1 and VDAC2 in all the human
175 tissues tested. Indeed, VDAC3 mRNA expression falls within a range of TPM (Transcripts Per
176 Kilobase Million) transcripts values higher than that of the other two isoforms. Even if the expression
177 of VDAC1 and VDAC2 transcripts falls in the same range, the latter isoform is the most expressed.
178 In Figure 2 VDACs mRNA levels are reported for some representative tissues. According to the
179 literature and other databases of transcripts expression, VDAC1 and VDAC2 are mainly represented
180 in bone marrow, brain, testis, heart, tongue. However, in FANTOM 5 project dataset the VDAC2
181 level is doubled compared to VDAC1. Although VDAC3 mRNA expression overcomes VDAC1 and
182 VDAC2, the tissues with a higher level of its expression are confirmed to be heart, testis, muscles.
183 The data emerging from this analysis highlight for the first time the prevalence of VDAC3 gene
184 transcription compared to other isoforms reflecting a higher promoter activity.

185 With this analysis, we can also confirm that VDAC isoforms are ubiquitously expressed in tissues
186 even if with different specificity for each isoform.

187

188

189 **VDAC isoforms comparative expression in HeLa cells**

190 VDAC isoforms transcription was analyzed in HeLa cells and a comparison of their expression level
191 was performed. mRNA of VDAC1 gene was established as reference gene and quantification of
192 VDAC2 and VDAC3 mRNA level was reported relative to VDAC1. In Figure 4 a, VDAC2 transcript
193 amount is slightly lower than VDAC1 mRNA showing a value of 0.78, while VDAC3 transcripts are
194 almost half of VDAC1 with a value of 0.39. VDAC3 mRNA is the less expressed transcript among
195 the three isoforms. The data obtained confirm VDAC transcription expression as revealed by GTEx
196 data analysis and previous experimental results obtained by us [34].

197

198 **VDACs genes transcriptional promoter activity**

199 A 600 bp genomic region encompassing the TSS of VDACs gene was identified as putative promoter
200 named P_{VDAC1} , P_{VDAC2} and P_{VDAC3} and utilized for experimental characterization. These sequences
201 were cloned in front of the Luciferase (Luc) reporter gene, to study the activity of the human VDACs
202 genes promoters in HeLa cells. Luciferase activity, driven by the indicated VDACs promoters was
203 compared among the three isoforms as shown in the histogram of Figure 4 b. Surprisingly VDAC1,
204 the most represented isoform holds the less active promoter which drives a transcriptional activation
205 10 and 8 folds lower than VDAC3 and VDAC2 promoters. These experimental results are in
206 agreement with the predominant transcriptional activity of VDAC3 and VDAC2 emerging from
207 FANTOM 5 project suggesting a mechanism of fine regulation of VDACs expression.

208

209 **Characterization of VDAC genes core promoters**

210 Very limited information is available regarding the core promoter organization of VDACs genes.
211 Using different predictive strategies through EPD, YAPP Eukaryotic Core Promoter Predictor and
212 ElemeNT, we built an overview of the most relevant core promoter elements captured with the higher
213 consensus match and functionally recommended scores (p-value $\geq 0,001$), which we schematically
214 represented for P_{VDAC1} (a), P_{VDAC2} (b), and P_{VDAC3} (c) (Fig. 5). The promoter region of each VDAC

215 isoform lacks a canonical TATA box, but contains the Initiator element (Inr), downstream promoter
216 element (DPE) and B recognition element (BRE). As typically observed in TATA-less promoters,
217 multiple GC-boxes are required and Inr and DPE are functionally analogous to the TATA box as they
218 cooperate for the binding of TFIID in the transcription [35]. In P_{VDAC2} (a) and P_{VDAC3} (c) a non-
219 canonical initiation site termed the TCT motif (polypyrimidine initiator) was identified. This
220 polypyrimidine stretch proximal to the 5' end of these genes is a target for translation regulation and
221 oxidative and metabolic stress, or cancer-induced differential translational regulation by the mTOR
222 pathway [36].

223

224 **Characterization of VDACs' transcriptional regulators**

225 Identifying the upstream regulators of VDAC genes will allow a better understanding of the biological
226 role that each isoform plays in the cell. Thus, VDAC genes were characterized for the TFBSs by
227 scanning the promoter sequences with three different bioinformatics tools (Genomatix, Jaspar,
228 UniBind) and the results were overlapped in order to find the most relevant TF families that regulate
229 VDAC genes expression. We used a search window of -400 to +200 bp around the TSS.

230 In Figure 6 a, histogram is reported showing every TFBS family found on the VDAC promoters'
231 sequences that were predicted by MatInspector software (Genomatix v3.10) and experimentally
232 validated by ChIP-Seq data (ENCODE project v3). The ChIP-Seq Peaks of V\$E2FF, V\$EGRF,
233 V\$KLFS, V\$NRF1, V\$MAZF, V\$SP1F, V\$ZF02, V\$ZF5F are numerically the most
234 overrepresented as highlighted by the bioinformatic prediction, confirming the importance of these
235 factors in the regulatory network of VDAC genes. These binding sites are known to participate in
236 several biological processes, such as cell growth, proliferation and differentiation, development,
237 inflammation and tumorigenesis [37-43]. Among them, V\$NRF1 is the master regulator of genes
238 encoding mitochondrial proteins and V\$E2FF is a family of factors involved in the control of the cell
239 cycle. The results of Figure 6 a were reorganized in a Venn chart showing the transcription factors

240 binding sites shared by VDACs promoter sequences and those exclusively present in each VDAC
 241 gene promoter, as reported by Genomatix analysis (Fig.6 b).

242 *Analysis of VDACs common TFBSs*

243 The overlap between Genomatix results and data extracted from JASPAR and UniBind databases
 244 highlights the occurrence of four families of shared TFBSs in promoter regions of VDAC genes. A
 245 comprehensive location of both sets of TFBSs was also extracted from ENCODE ChIP-seq peaks
 246 (Table 1). The detection of common TFBS clusters indicates that these different classes of TFs
 247 participate in many similar activities prevalently involved in cell proliferation and differentiation,
 248 apoptosis and metabolism regulation. Therefore, it is possible to divide different classes of TFs
 249 involved in the control of VDAC genes in three functional categories: the first one is represented by
 250 V\$E2FF (E2F-myc activator/cell cycle) transcription factors, affecting various processes of cell cycle
 251 regulation [44]. The second group includes members of V\$EBOX (E-box binding factors) and
 252 V\$KLFS (Krueppel like transcription factors) families, which are essential transcription factors that
 253 regulate a large number of cellular processes, such as metabolism, cell proliferation, differentiation,
 254 apoptosis, and cell transformation [45, 46]. The third group comprises V\$NRF1 (Nuclear respiratory
 255 factor 1) family, closely connected with mitochondrial biogenesis, DNA damage signalling, and
 256 tumour metabolism [47-49].

257 **Table 1.** VDACs common TFBSs

Matrix Family	Description	RATE OF FREQUENCY IN DB								
		P _{VDAC1}			P _{VDAC2}			P _{VDAC3}		
		Genomatix	Jaspar	Unibind	Genomatix	Jaspar	Unibind	Genomatix	Jaspar	Unibind
V\$E2FF	E2F-myc activator/cell cycle regulator	✓	✓	✓	✓	✓	✓	✓	✓	-
V\$EBOX	E-box binding factors	✓	✓	✓	✓	-	-	✓	✓	✓
V\$KLFS	Krueppel like transcription factors	✓	✓	✓	✓	✓	✓	✓	✓	✓
V\$NRF1	Nuclear respiratory factor 1	✓	✓	✓	✓	✓	✓	✓	✓	✓

258

259 *Analysis of VDACs unique TFBSs*

260 The data extracted from Genomatix, Jaspar, and UniBind, were collected to obtain information about
 261 families of TFBS exclusively found in each promoter sequence: they thus define the unique TFs
 262 controlling each single VDAC isoform. We found in the P_{VDAC1} sequence (Table 2) four unique TFBS
 263 families: V\$AHRR (AHR-arnet heterodimers and AHR-related factors) which is required, together
 264 with HIF-1 α factor, for the cell response to hypoxia [50]; V\$SETSF (Human and murine ETS1 factors)
 265 that includes NRF2, a regulator of mitochondrial biogenesis and redox homeostasis [51]; V\$HEAT
 266 (heat shock factors) a family of proteins crucial for cell stress response [52]; V\$PBXC (PBX-MEIS
 267 complexes), also known as pre-B cell leukemia family, that includes regulators of cell development,
 268 survival, invasion and proliferation [53].

269 **Table 2.** VDAC1 unique TFBSs

		RATE OF FREQUENCY IN DB		
Matrix Family	Description	P_{VDAC1}		
		<i>Genomatix</i>	<i>Jaspar</i>	<i>UniBind</i>
V\$AHRR	AHR-arnet heterodimers and AHR-related factors	-	-	✓
V\$SETSF	Human and murine ETS1 factors	✓	-	-
V\$HEAT	Heat shock factors	✓	-	-
V\$PBXC	PBX - MEIS complexes	-	-	✓

270
 271 As concerning P_{VDAC2} sequence (Table 3), we identified several binding sites recognized by regulators
 272 know to be associated with the nervous system development and general core promoter elements.
 273 Among them: V\$BEDF (BED subclass of zinc-finger proteins) includes ZBED which controls cell
 274 growth and differentiation in cone photoreceptors and Müller cells of human retina [54]; V\$BRAC
 275 (Brachyury gene, mesoderm developmental factor), is involved in the commitment of T helper (Th)
 276 cells [55]; V\$CLOX (CLOX and CLOX homology (CDP) factors), a crucial regulator of the neuronal
 277 differentiation in the brain [56]; V\$MEF3 (MEF3 binding sites) a family that includes regulators of
 278 skeletal muscle development [57]; V\$NEUR (NeuroD, Beta2, HLH domain), comprising the basic
 279 helix-loop-helix factors *Ascl1* and *OLIG2* involved in neural development and differentiation [58];
 280 TF2B (RNA polymerase II transcription factor II B) a core promoter element [59]; V\$ZFX (Zfx
 281 and Zfy - transcription factors), a family of transcription factors implicated in mammalian sex de

282 Termination [60].

283

284 **Table 3.** VDACC2 unique TFBSs

Matrix Family	Description	RATE OF FREQUENCY IN DB		
		<i>Genomatix</i>	<i>Jaspar</i>	<i>UniBind</i>
V\$BEDF	BED subclass of zinc-finger proteins	✓	-	-
V\$BRAC	Brachyury gene, mesoderm developmental factor	-	-	✓
V\$CLOX	CLOX and CLOX homology (CDP) factors	-	-	✓
V\$MEF3	MEF3 binding sites	✓	-	-
V\$NEUR	NeuroD, Beta2, HLH domain	✓	-	-
O\$TF2B	RNA polymerase II transcription factor II B	✓	-	-
V\$ZFX	Zfx and Zfy - transcription factors	-	-	✓

285

286 The results of P_{VDACC3} analysis (Table 4) showed a distribution of binding sites for TFs involved in the
 287 control of various cellular processes including cell differentiation, proliferation, apoptosis, and
 288 gametogenesis: V\$BCL6 (BED subclass of zinc-finger proteins), a critical regulator of B cell
 289 differentiation [61]; V\$CDXF (Vertebrate caudal related homeodomain protein) involved in
 290 development and maintenance of trophoderm [62]; V\$FOX (Forkhead (FKH)/ Forkhead box
 291 (Fox)), including important regulators of development, organogenesis, metabolism and cell
 292 homeostasis [63]; V\$SOHLH (Spermatogenesis and oogenesis basic helix-loop-helix) transcription
 293 regulators of male and female germline differentiation [64]; V\$HMG (High-Mobility Group family),
 294 including factors that regulate neuronal differentiation and also play important roles in tumorigenesis
 295 [65]; V\$HOMF (Homeodomain transcription factors) involved in central nervous development [66];
 296 V\$IRFF (Interferon regulatory factors) required for differentiation of hematopoietic cells [67];
 297 V\$LBXF (Ladybird homeobox (lhx) gene family) that plays a critical role in embryonic neurogenesis
 298 and myogenesis and in muscle mass determination [68]; V\$MYBL (cellular and viral myb-like
 299 transcriptional regulators) that controls cell cycle progression, survival and differentiation [69];
 300 V\$SMAD (Vertebrate SMAD family of transcription factors) that includes factors responsible of

301 several cellular processes, including proliferation, differentiation, apoptosis, migration, as well as
 302 cancer initiation and progression [70]; V\$XBBF (X-box binding factors) family involved in the
 303 control of development and maintenance of the endoplasmic reticulum (ER) in multiple secretory cell
 304 lineages [71].

305 **Table 4.** VDAC3 unique TFBSs

Matrix Family	Description	RATE OF FREQUENCY IN DB		
		P_{VDAC3}		
		<i>Genomatix</i>	<i>Jaspar</i>	<i>UniBind</i>
V\$BCL6	POZ domain zinc finger expressed in B-Cells	-	-	✓
V\$CDXF	Vertebrate caudal related homeodomain protein	-	-	✓
V\$FOX	Forkhead (FKH)/ Forkhead box (Fox)	-	-	✓
V\$SOHLH	Spermatogenesis and oogenesis basic helix-loop-helix	-	✓	-
V\$HMG	HMG family	✓	-	-
V\$HOMF	Homeodomain transcription factors	✓	✓	-
V\$IRFF	Interferon regulatory factors	-	-	✓
V\$LBXF	Ladybird homeobox (lhx) gene family	-	✓	-
V\$MYBL	Cellular and viral myb-like transcriptional regulators	-	✓	-
V\$SMAD	Vertebrate SMAD family of transcription factors	-	✓	-
V\$XBBF	X-box binding factors	✓	-	-

306
 307 In Figure 7 (a-c) a magnification of VDACs promoters analyzed from UCSC Genome Browser is
 308 overlapped with experimental data proving the transcriptional activity of this genomic region. Based
 309 on Genomatix results on distinct and shared TFBSs at promoter regions of P_{VDAC1} , P_{VDAC2} , and P_{VDAC3} ,
 310 a comprehensive location of both sets of TFBSs was extracted from ENCODE ChIP-seq peaks. These
 311 findings are also supported by TFBSs enrichment analyses from JASPAR and UniBind database. In
 312 the graphical view, the most interesting peaks of TFBS found, are located in overlapping positions of
 313 the promoter for different cell lines. Moreover, these validated TFBSs fall in the genomic region
 314 corresponding to VDACs promoter studied in this work.

315 The determination of common TFBSs appear to corroborate shared biological properties, as well as
 316 a high degree of functional conservation and cooperation among the three isoforms, while the

317 mapping of unique TFBSs robustly supported by different databases suggest a different biological
318 role.

319 **Discussion**

320 To understand the specialized biological role of VDACs isoforms, simultaneously expressed in cells,
321 we performed a characterization of VDACs transcripts expression and promoters' structure and
322 function. To have a general but reliable picture of VDAC genes structure, expression, and regulation,
323 we undertook a study of VDACs isoforms in the main available public resource reporting high
324 throughput data of international collaborative projects.

325 *Structure of VDAC genes, transcripts and promoters*

326 First of all, a general view of VDAC genes, transcripts variants, and promoter regions feature by in
327 silico analysis through UCSC genome browser is shown. For each VDAC genes, several different
328 transcripts splice variants were identified varying not in the coding region but mainly in their 5'-UTR
329 and 3'-UTR length. Other variants are processed transcripts, other present retained intron and for
330 VDAC3 two are involved in nonsense-mediated decay mechanism. The variability on the UTR
331 sequences let to hypothesize differentiated mechanism of transcript regulation and expression context
332 for each variant. The 3'-UTR sequence may be a target of translation regulation by miRNA or
333 interference. Many publications indeed reported the identification of miRNA molecules targeting all
334 three VDACs transcripts but in particular VDAC1 [72]. The 5'-UTR region variability might be
335 associated with alternative promoter usage and activation in a different expression context. However,
336 no information is available on the human VDACs promoter and/or other regulative regions to explain
337 transcripts expression.

338 *VDAC expression in Gene Expression Atlas repository*

339 For this reason, we wanted to focus our study on the characterization of the main promoter driving
340 each VDACs genes transcripts expression. First of all, we selected from Gene Expression Atlas

341 repository, the data derived from the RNA-seq CAGE RIKEN FANTOM 5' project and the RNA-
342 seq GTEx projects.

343 Generally, although the expression profile of VDACs transcripts presents a differentiated level in
344 different tissues or cells types, all three isoforms are ubiquitously expressed [2]. The level of VDAC1
345 and VDAC2 transcripts is comparable, while VDAC3 is always less expressed [34]. Surprisingly,
346 analyzing the data set of FANTOM 5 project we found that VDAC3 transcripts expression overcome
347 VDAC2 but in particular VDAC1 which results to be scarcely represented in all tissues compared to
348 the other VDACs. The special version of RNA-seq methodology based on cap analysis of gene
349 expression adopted by the FANTOM5 consortium allowed to identify active TSS located on the 5'-
350 end of transcribed mRNA which are not necessarily associated to a full length and/or protein coding
351 transcript. Based on this evidence, we selected the main promoter region found in Eukaryotic
352 Promoter Database EPD associated to the main protein-coding transcript and we confirmed by
353 luciferase reporter assay the highest transcriptional activity of VDAC3 promoter and the VDAC1
354 which is on the contrary the less active. These interesting results suggest a mechanism of more
355 complex and coordinated regulation of VDACs transcripts expression in order to enhance the most
356 represented and functional VDAC1 isoform and/or repress VDAC3. However, the higher promoter
357 activity of VDAC3 might be also interpreted as a potentiality maintained by the cells to promptly
358 respond to a particular and still unknown stimulation through VDAC3 increased expression in
359 specific conditions.

360 *VDAC genes core promoters*

361 With the aim to explore the mechanism of VDAC transcription regulation, we started a systematic
362 analysis of human VDAC genes promoters to highlight their structural and functional features.
363 VDACs genes core promoter organization is similar to most of TATA-less human core promoters of
364 ubiquitously expressed genes. Abundant GC regions, alternative binding sites Inr, DPE and BRE for
365 the basal transcription factors take over the function of TATA box sequence. Moreover, VDACs
366 genes, as most of human protein-coding genes lacking TATA-box, own a long 5'-UTR region

367 suggesting the presence of alternative TSS employed for expression of distinct products in different
368 contexts or tissues. As reported in the VDACS genes structure organization, the occurrence of several
369 transcripts, could explain their expression associated with different conditions.

370

371 *Transcription factors binding sites common to any VDAC gene*

372 We also characterized the main transcription factors regulating the activity of VDAC promoter
373 regions, looking for the transcription factors binding sites (TFBSs). The information we gained by
374 bioinformatic analysis, suggested the central role of VDAC protein expression in regulating
375 mitochondrial function in fundamental cell processes. We recognized TFBS shared by the three
376 VDACS promoters, as well as single promoters' unique sites. Among the common ones, the majority
377 of identified TFs classes belong to the E2FF, NRF1, SP1, KLFS, EBOX families which participate
378 in many similar activities but are prevalently involved in cell proliferation and differentiation,
379 apoptosis and metabolism regulation [37-43]. TFBS for E2FF and NRF1 transcription factor family
380 members are also numerically the most represented on all the three VDACS promoters. VDACS
381 promoters are mainly characterized by a large number of recognition sites for E2FF and NRF1
382 transcription factors, which were found associated by chromatin immunoprecipitations with
383 microarrays (ChIP-on-chip) to a significant subset of genes implicated in mitochondrial biogenesis
384 and metabolism, other than mitosis, cytokinesis, cell cycle control, grow, proliferation [73]. Many
385 identified TFBS are located in the proximal core promoter acting as co-regulators for general
386 transcription factors activation and chromatin regulation. In particular, some of them, SP1, KLFS,
387 EBOX, NRF1 rich in GC content have an important role in epigenetic control of promoter suggesting
388 a more complex regulation of this genes [74].

389 *Transcription factors binding sites specific to each VDAC gene*

390 Search for unique transcription factor binding sites on the promoters of VDAC isoforms, allowed us
391 to hypothesize their involvement in specialized biological functions. However, the transcription
392 factors specific for each VDAC genes are always correlated to essential functions ensuring cell

393 survival and functionality. In general, these processes require a noteworthy energy cost: metabolism
394 maintenance, development, organogenesis, dysfunction of mitochondria in pathology, are some
395 examples.

396 The families of transcription regulators identified as unique in VDAC1 promoter suggests that this
397 isoform was probably selected by evolutionary process to have the prevalent role of channel protein
398 in the mitochondrial outer membrane in physiological context and in particular when altered
399 conditions force the cells to restore the mitochondria energetic balance [75]. These observations are
400 corroborated by several experimental evidence showing the involvement of VDAC1 in regulating
401 many cellular and mitochondrial events in pathology or stress conditions through the interaction with
402 specific protein [76].

403 VDAC2 was indicated as the isoform carrying out channel function and governing apoptosis and
404 autophagy in various contexts [5]. Analysis of VDAC2 promoter highlighted the presence of different
405 factors specially involved in development of specialized tissues and organogenesis process as unique
406 among VDACs promoters. Most of these factors are related to nervous system genesis and
407 development.

408 VDAC3 is controlled by the most active promoter: it is particularly rich of GC repetitions, suggesting
409 an epigenetic control mechanism able to reduce the expression of transcripts. Factors binding sites
410 found in VDAC3 promoter belong to various families but those involved in development of germinal
411 tissues, organogenesis and sex determination are the most abundant. Also in this case, the
412 experimental evidence reported in the literature confirms the crucial role of VDAC3 in fertility [13].

413

414 **Conclusion**

415 In conclusion we proposed a general overview of the structural and functional organization of VDACs
416 isoforms promoters cross-referencing public available data source, bioinformatics prediction and
417 experimental data. From this analysis, it emerges the essential function of the family of VDAC
418 proteins in the regulation of mitochondrial energetic metabolism in physiological and pathological

419 cell life. Moreover, we shed some new light on the molecular mechanisms that explain the differences
420 among three VDAC isoforms. It is becoming increasingly clear that the most known specialized
421 functions of each VDAC isoforms are connected with the organization of the "button room" that
422 decides the transcriptional activity of their genes and were produced by evolution.

423

424 **Materials and Methods**

425

426 **Bioinformatic analysis of promoter region**

427 Human promoter retrieval for *hVDAC1* (NM_003374), *hVDAC2* (NM_001324088) and *hVDAC3*
428 (NM_005662) genes was carried out by high-quality promoter resource EPDnew version 006
429 (<https://epd.epfl.ch>). For study purposes, P_{VDAC1} (chr5:133,340,230-133,340,830; hg19) P_{VDAC2}
430 (chr10:76,970,184-76,970,784; hg19) and P_{VDAC3} (chr8:42,248,998-42,249,598; hg19) are the
431 promoter sequences extended from -400 bp to +200 bp relative to annotated Transcription Start Site
432 (TSS) of basal EPD promoter sequences (VDAC1_1; VDAC2_1; VDAC3_1). Tools used to scan for
433 canonical core promoter elements and synergistic combinations were EPD Promoter Elements Page,
434 YAPP Eukaryotic Core Promoter Predictor ([http://www.bioinformatics.org/yapp/cgi-](http://www.bioinformatics.org/yapp/cgi-bin/yapp_intro.cgi)
435 [bin/yapp_intro.cgi](http://www.bioinformatics.org/yapp/cgi-bin/yapp_intro.cgi)), and ElemeNT (<http://lifefaculty.biu.ac.il/gershon-tamar/index.php/resources>).
436 Analysis of Transcription Factor Binding Site (TFBS) clusters was done by Genomatix software suite
437 (Genomatix v3.10). *MatInspector* application was used to identify potential binding sites for
438 transcription factors (TFBSs) in input sequence using the Matrix Family Library version 11.0 for core
439 promoter elements in vertebrates with a fixed matrix similarity threshold of 0.85 [77].
440 TFBSs enrichment analyses was also performed using JASPAR database, a carefully selected DB of
441 position-specific scoring matrices derived from experimentally validated TFBS [78], and UniBind
442 database encompassing predicted direct TF–DNA interactions derived from PWMs covering >2% of
443 the human genome [79]. In view of implementing the TFBS clusters analysis, all information relevant
444 to the genomic structure and DNA regulatory elements related to three VDAC isoforms were

445 investigated using UCSC Genome Browser (<https://genome.ucsc.edu>). DNA regulation tracks of
446 UCSC Genome Browser and some information of promoter sequence and TFBS predictions are
447 currently available on GRCh37/hg19.

448

449 **Gene expression data retrieval**

450 Gene expression results were collected from Gene Expression Atlas of EMBL-EBI open science
451 resource (<https://www.ebi.ac.uk/gxa/home>), a database of RNA-seq, microarray and, proteomics data
452 manually curated and analyzed through standardized analysis pipelines. The Baseline Atlas database
453 containing the RNA-seq experiments regarding expression of gene in tissues under physiological
454 conditions was consulted and data from Genotype-Tissue-Expression (GTEx) [32] and Functional
455 ANnotation of the Mammalian Genome 5 (FANTOM) project [33] were selected for VDAC isoforms
456 expression analysis. The data are displayed in a heatmap with different colour representing a range
457 of TPM mRNA expression level. Transcripts expression level of the three VDACs gene were selected
458 for the most common tissues and represented by a histogram and reported in a table.

459

460 **Quantitative Real-time PCR**

461 0.6×10^6 of HeLa cells were plated in 25 cm² flasks. After 48h of incubation total RNA was extracted
462 using "ReliaPrep RNA cell mini-prep system" (Promega) according to manufacturer's instructions.
463 RNA concentration and purity were measured by a spectrophotometer and 2 ug were used to
464 synthesize cDNA by QuantiTect Reverse Transcription kit (Qiagen). Real-time amplification was
465 performed in a Mastercycler EP Realplex (Eppendorf) in 96-well plates. The reaction mixture
466 contained 1.5 ul cDNA, 0.2 uM gene specific primers pairs (hVDAC1, hVDAC2, hVDAC3, β -actin)
467 and 12.5 ul of master mix (QuantiFast SYBR Green PCR kit, Qiagen). Three independent
468 experiments of quantitative real-time were performed in triplicate for each sample. Analysis of
469 relative expression level was performed by the $\Delta\Delta C_t$ method using the housekeeping β -actin gene as
470 internal calibrator and VDAC1 gene as reference.

471 **Plasmid constructs**

472 A putative promoter region of 600bp encompassing the TSS of the human VDACs genes was selected
473 from GenBank and cloned into pGL3 basic vector (Promega) for transcriptional activity study. The
474 construct P_{VDAC1} contain the sequence (chr5:133,340,230-133,340,830; hg19) derived from VDAC1
475 NM_003374, P_{VDAC2} contain the genomic trait (chr10:76,970,184-76,970,784; hg19) from VDAC2
476 NM_001324088 and P_{VDAC3} the sequence (chr8:42,248,998-42,249,598; hg19) of VDAC3
477 NM_005662.

478

479 **Promoter reporter assay**

480 HeLa cells were plated at density of 0.3×10^6 cells/well in a 6 wells plate. After 24h, cells were
481 transfected with 800 ng of pGL3 constructs and 20 ng of pRL-TK renilla reporter vector by Transfast
482 transfection reagent according to manufacturer's protocol (Promega) and after 48h cells were lysed.
483 Luciferase activity of cell lysate transfected with pGL3 promoter constructs was detected with the
484 Dual Luciferase Assay (Promega) according to the manufacturer's instructions. Activity of firefly
485 luciferase relative to renilla luciferase was expressed in relative luminescence units (RLU). Variation
486 of luminescence units of treated samples relative to control, were indicated as fold increase (FI).

487

488

489 **Abbreviations**

490

491 AHRR (AHR-arnt heterodimers and AHR-related factors)

492 BCL6 (BED subclass of zinc-finger proteins)

493 BEDF (BED subclass of zinc-finger proteins)

494 BRAC (Brachyury gene, mesoderm developmental factor)

495 BRE (B recognition element)

496 CDXF (Vertebrate caudal related homeodomain protein)

497 ChIP-on-chip (CHromatin ImmunoPrecipitations with microarrays)

498 CLOX (CLOX and CLOX homology (CDP) factors)

499 DPE (Downstream promoter element);

500 E2FF (E2F-myc activator/cell cycle);

501 EBOX (E-box binding factors)

502 ER (Endoplasmic Reticulum)

503 ETSF (Human and murine ETS1 factors)

504 FANTOM (Functional ANnotation of the Mammalian Genome)

505 FOX (Forkhead (FKH)/ Forkhead box (Fox)

506 GTEX (Genotype-Tissue Expression)

507 HEAT (heat shock factors)

508 HMG (High-Mobility Group family)

- 509 HOMF (Homeodomain transcription factors)
- 510 Inr (Initiator Element)
- 511 IRFF (Interferon regulatory factors)
- 512 KLFS (Krueppel like transcription factors)
- 513 LBXF (Ladybird homeobox (lhx) gene family)
- 514 MEF3 (MEF3 binding sites)
- 515 MYBL (cellular and viral myb-like transcriptional regulators)
- 516 NEUR (NeuroD, Beta2, HLH domain)
- 517 NRF1 (Nuclear respiratory factor 1)
- 518 PBXC (PBX-MEIS complexes)
- 519 SMAD (Vertebrate SMAD family of transcription factors)
- 520 SOHLH (Spermatogenesis and oogenesis basic helix-loop-helix)
- 521 TF2B (RNA polymerase II transcription factor II B)
- 522 TFBSs (Transcription Factor Binding Sites);
- 523 TSS (Transcription Start Site)
- 524 VDAC (Voltage-Dependent Anion selective Channel);
- 525 XBBF (X-box binding factors)
- 526 ZFXY (Zfx and Zfy - transcription factors)
- 527
- 528

529 **Figure legends**

530

531 **Figure 1. Human *VDAC* isoforms genes structure and function.**

532 Overview of gene structure of human *VDAC* isoforms and their most relevant functional and
533 structural sites. (a) *hVDAC1* gene location on Chr5:133,340,230-133,340,830 (GRCh37/hg19) from
534 UCSC Genome Browser; (b) *hVDAC2* gene location on Chr10:76,970,184-76,970,784; hg19; (c)
535 *hVDAC3* gene location on Chr8:42,248,998-42,249,598; hg19. In each panel a black box encloses the
536 600bp promoter sequence indicated as P_{VDAC1}, P_{VDAC2} and P_{VDAC3}, respectively, and aligned with the
537 annotated sequence from EPDnew (v.006). This allows highlighting the profile of transcriptional
538 activity of the gene promoter region by CpG island identification, levels of enrichment of the
539 H3K4me1 and H3K4me3 histone marks, and RNA Pol2 and Chromatin State Segmentation ChIP-
540 seq data. Functional elements of Chromatin state segmentation by HMM of nine different cell lines
541 are identified by different colours as follows: bright red: active promoter; light red: weak promoter;
542 orange: strong enhancer; yellow: weak/poised enhancer; blue: insulator; dark green: transcriptional
543 transition/elongation; light green: transcriptional transcribed.

544

545 **Figure 2. Human *VDAC* genes expression by Genotype-Tissues-Expression (GTEx) database.**

546 RNA-seq data from Genotype-Tissues-Expression (GTEx) project were collected from Gene
547 Expression Atlas repository where all data are manually curated and subject to standardized analysis
548 pipelines. The data are displayed in a heatmap (a) with different colours representing a range of TPM
549 mRNA expression level: grey (expression level is below cutoff - 0.5 TPM or FPKM); light blue
550 (expression level is low - between 0.5 to 10 TPM or FPKM); medium blue (expression level is
551 medium - between 11 to 1000 TPM or FPKM); dark blue (expression level is high - more than 1000
552 TPM or FPKM); white box (no data available). In the panel b the specific expression values of each
553 human *VDAC* isoforms, for representative tissues, are reported.

554

555 **Figure 3. Human VDAC genes expression by RIKEN FANTOM 5 project.**

556 RNA-seq CAGE data from RIKEN FANTOM 5 project were collected from Gene Expression Atlas
557 repository where all data are manually curated and subject to standardized analysis pipelines. The
558 data are displayed in a heatmap (**a**) with different colours representing a range of TPM mRNA
559 expression level as described for Figure 2. In the Panel **b** the specific expression values of each human
560 VDAC isoforms, for representative tissues, are reported.

561

562 **Figure 4. Experimental analysis of human VDAC gene expression and their promoter activity**
563 **in HeLa cells.**

564 **a)** Human VDAC genes expression. VDAC genes expression was detected by Real Time PCR as
565 described in methods. After normalization with the housekeeping gene b-actin, the variation of
566 hVDAC2 and hVDAC3 transcripts was expressed using human VDAC1 as reference. The $\Delta\Delta C_t$
567 method was applied.

568 **b)** VDAC promoters activity detection. To study the promoters activity, 600 bp sequence
569 encompassing the TSS (from -400 to +200 in the gene sequence) were placed upstream the luciferase
570 gene in pGL3 plasmid. The assay was performed in HeLa cells transfected with P_{vdac1} -pGL3, P_{vdac2} -
571 pGL3, P_{vdac3} -pGL3 constructs after 48h of transfection. Luciferase activity of cell lysates was
572 calculated by referring to empty-pGL3 transfected cells and following normalization with *Renilla*
573 activity.

574 Three independent experiments were performed and results statistically analyzed by one-way
575 ANOVA. A value of $P < 0,05$ was taken as significant.

576

577 **Figure 5. Canonical core promoter elements of human VDAC isoforms.** The results of core
578 promoter elements identified for *hVDAC1*, *hVDAC2* and *hVDAC3* genes by predictive tools are the
579 sequence stretches with a high scoring consensus based on position weight matrix (PWM). (**a**) P_{VDAC1}
580 (chr5:133,340,230-133,340,830; hg19) encompasses an Inr element (at -261 bp), two GC-boxes (at -

581 85 bp; -49 bp), five BRE motifs (at -255 bp; -217 bp; -78 bp; -42 bp; -27 bp), and two DPE motifs (at
582 -298 bp; -266). **(b)** P_{VDAC2} (chr10:76,970,184-76,970,784; hg19) encompasses a TCT motif, as
583 alternative Inr (at +2 bp), Inr element (at +8 bp), two BRE motifs (at + 93 bp; +119 bp), a DPE motif
584 (at -173 bp). **(c)** P_{VDAC3} (chr8:42,248,998-42,249,598; hg19) encompasses three Inr elements (at -205
585 bp; - 8 bp; + 77 bp), a TCT (at -329 bp), a DPE (at -1 bp) and a BRE (at + 170 bp).
586 TSS site is indicated by a thick red arrow. Nucleotide sequence before TSS is shown in lowercase.

587

588 **Figure 6. Identification of ChIP-seq peak regions in the human $VDAC$ promoters.**

589 **a)** The histogram shows the number of TFBS experimentally validated by ChIP-Seq data (ENCODE
590 project v3) among those predicted by the software Genomatix (MatInspector) in P_{VDAC1} , P_{VDAC2} and
591 P_{VDAC3} sequences. **b)** Venn diagram showing the number of common and unique predicted binding
592 sites that overlap with a ChIP-Seq region in P_{VDAC1} , P_{VDAC2} and P_{VDAC3} , based on Genomatix analysis.

593

594 **Figure 7. Identification of common and unique transcription factor binding site clusters of**
595 **$VDACs$ promoter sequences.**

596 Distribution of a common set (enclosed in a blue box) and specific sets (enclosed in a red box) of
597 Transcription Factors binding sites (TFBS) in $VDAC$ isoforms promoters as reported in different cell
598 lines by ChIP-Seq analysis in ENCODE Project (shown as colour vertical bars in the gray segments).

599 **a)** $hVDAC1$, **b)** $hVDAC2$, and **c)** $hVDAC3$.

600

601

602

603

604

605

606 **References**

- 607 1. Shoshan-Barmatz V, De Pinto V, Zweckstetter M, Raviv Z, Keinan N, Arbel N. VDAC, a multi-
608 functional mitochondrial protein regulating cell life and death. *Molecular aspects of medicine*.
609 2010 Jun;31(3):227-85. PubMed PMID: 20346371.
- 610 2. Messina A, Reina S, Guarino F, De Pinto V. VDAC isoforms in mammals. *Biochimica et*
611 *biophysica acta*. 2012 Jun;1818(6):1466-76. PubMed PMID: 22020053.
- 612 3. Colombini M. VDAC: the channel at the interface between mitochondria and the cytosol.
613 *Molecular and cellular biochemistry*. 2004 Jan-Feb;256-257(1-2):107-15. PubMed PMID:
614 14977174.
- 615 4. Benz R. Permeation of Hydrophilic Solutes through Mitochondrial Outer Membranes - Review on
616 Mitochondrial Porins. *Bba-Rev Biomembranes*. 1994 Jun 29;1197(2):167-96. PubMed PMID:
617 WOS:A1994NX15200004. English.
- 618 5. Naghdi S, Hajnoczky G. VDAC2-specific cellular functions and the underlying structure.
619 *Biochimica et biophysica acta*. 2016 Oct;1863(10):2503-14. PubMed PMID: 27116927. Pubmed
620 Central PMCID: 5092071.
- 621 6. Checchetto V, Reina S, Magri A, Szabo I, De Pinto V. Recombinant human voltage dependent
622 anion selective channel isoform 3 (hVDAC3) forms pores with a very small conductance. *Cellular*
623 *physiology and biochemistry : international journal of experimental cellular physiology,*
624 *biochemistry, and pharmacology*. 2014;34(3):842-53. PubMed PMID: 25171321.
- 625 7. Queralt-Martin M, Bergdoll L, Teijido O, Munshi N, Jacobs D, Kuszak AJ, et al. A lower affinity
626 to cytosolic proteins reveals VDAC3 isoform-specific role in mitochondrial biology. *The Journal*
627 *of general physiology*. 2020 Feb 3;152(2). PubMed PMID: 31935282. Pubmed Central PMCID:
628 7062508.

- 629 8. Sampson MJ, Lovell RS, Davison DB, Craigen WJ. A novel mouse mitochondrial voltage-
630 dependent anion channel gene localizes to chromosome 8. *Genomics*. 1996 Aug 15;36(1):192-6.
631 PubMed PMID: 8812436.
- 632 9. Neumann D, Buckers J, Kastrup L, Hell SW, Jakobs S. Two-color STED microscopy reveals
633 different degrees of colocalization between hexokinase-I and the three human VDAC isoforms.
634 *PMC biophysics*. 2010 Mar 5;3(1):4. PubMed PMID: 20205711. Pubmed Central PMCID:
635 2838807.
- 636 10. Reina S, Palermo V, Guarnera A, Guarino F, Messina A, Mazzoni C, et al. Swapping of the N-
637 terminus of VDAC1 with VDAC3 restores full activity of the channel and confers anti-aging
638 features to the cell. *FEBS letters*. 2010 Jul 2;584(13):2837-44. PubMed PMID: 20434446.
- 639 11. Anfous K, Armstrong DD, Craigen WJ. Altered mitochondrial sensitivity for ADP and
640 maintenance of creatine-stimulated respiration in oxidative striated muscles from VDAC1-
641 deficient mice. *The Journal of biological chemistry*. 2001 Jan 19;276(3):1954-60. PubMed PMID:
642 11044447.
- 643 12. Cheng EH, Sheiko TV, Fisher JK, Craigen WJ, Korsmeyer SJ. VDAC2 inhibits BAK activation
644 and mitochondrial apoptosis. *Science*. 2003 Jul 25;301(5632):513-7. PubMed PMID: 12881569.
- 645 13. Sampson MJ, Decker WK, Beaudet AL, Ruitenbeek W, Armstrong D, Hicks MJ, et al. Immotile
646 sperm and infertility in mice lacking mitochondrial voltage-dependent anion channel type 3. *The*
647 *Journal of biological chemistry*. 2001 Oct 19;276(42):39206-12. PubMed PMID: 11507092.
- 648 14. Menzel VA, Cassara MC, Benz R, de Pinto V, Messina A, Cunsolo V, et al. Molecular and
649 functional characterization of VDAC2 purified from mammal spermatozoa. *Bioscience reports*.
650 2009 Jul 22;29(6):351-62. PubMed PMID: 18976238.
- 651 15. Manczak M, Sheiko T, Craigen WJ, Reddy PH. Reduced VDAC1 protects against Alzheimer's
652 disease, mitochondria, and synaptic deficiencies. *Journal of Alzheimer's disease : JAD*.
653 2013;37(4):679-90. PubMed PMID: 23948905. Pubmed Central PMCID: 3925364.

- 654 16. Nowak G, Megyesi J, Craigen WJ. Deletion of VDAC1 Hinders Recovery of Mitochondrial and
655 Renal Functions After Acute Kidney Injury. *Biomolecules*. 2020 Apr 10;10(4). PubMed PMID:
656 32290153. Pubmed Central PMCID: 7226369.
- 657 17. Huizing M, Ruitenbeek W, Thinnes FP, DePinto V, Wendel U, Trijbels FJ, et al. Deficiency of
658 the voltage-dependent anion channel: a novel cause of mitochondriopathy. *Pediatric research*.
659 1996 May;39(5):760-5. PubMed PMID: 8726225.
- 660 18. Huizing MR, W.; Thinnes, F.; De Pinto, V. Deficiency of the Voltage-Dependent Anion Channel
661 (VDAC): a novel cause of mitochondrial myopathies. *The Lancet*. 1994;344:762.
- 662 19. Baines CP, Kaiser RA, Sheiko T, Craigen WJ, Molkentin JD. Voltage-dependent anion channels
663 are dispensable for mitochondrial-dependent cell death. *Nature cell biology*. 2007 May;9(5):550-
664 5. PubMed PMID: 17417626. Pubmed Central PMCID: 2680246.
- 665 20. Reina S, Pittala MGG, Guarino F, Messina A, De Pinto V, Foti S, et al. Cysteine Oxidations in
666 Mitochondrial Membrane Proteins: The Case of VDAC Isoforms in Mammals. *Frontiers in cell
667 and developmental biology*. 2020;8:397. PubMed PMID: 32582695. Pubmed Central PMCID:
668 7287182.
- 669 21. Saletti R, Reina S, Pittala MGG, Magri A, Cunsolo V, Foti S, et al. Post-translational
670 modifications of VDAC1 and VDAC2 cysteines from rat liver mitochondria. *Biochimica et
671 biophysica acta Bioenergetics*. 2018 Sep;1859(9):806-16. PubMed PMID: 29890122.
- 672 22. Oliva M, De Pinto V, Barsanti P, Caggese C. A genetic analysis of the porin gene encoding a
673 voltage-dependent anion channel protein in *Drosophila melanogaster*. *Molecular genetics and
674 genomics* : MGG. 2002 Aug;267(6):746-56. PubMed PMID: 12207222.
- 675 23. Magri A, Di Rosa MC, Orlandi I, Guarino F, Reina S, Guarnaccia M, et al. Deletion of Voltage-
676 Dependent Anion Channel 1 knocks mitochondria down triggering metabolic rewiring in yeast.
677 *Cellular and molecular life sciences* : CMLS. 2019 Oct 26. PubMed PMID: 31655859.

- 678 24. Specchia V, Guarino F, Messina A, Bozzetti MP, De Pinto V. Porin isoform 2 has a different
679 localization in *Drosophila melanogaster* ovaries than porin 1. *Journal of bioenergetics and*
680 *biomembranes*. 2008 Jun;40(3):219-26. PubMed PMID: 18686020.
- 681 25. Hinsch KD, Asmarinah, Hinsch E, Konrad L. VDAC2 (porin-2) expression pattern and
682 localization in the bovine testis. *Biochimica et biophysica acta*. 2001 Apr 16;1518(3):329-33.
683 PubMed PMID: 11311949.
- 684 26. Pan L, Qiu D, Li J, Li J, Xu P, Zhao D, et al. Idiopathic male infertility in the Han population in
685 China is affected by polymorphism in the VDAC2 gene. *Oncotarget*. 2016 Dec 13;7(50):82594-
686 601. PubMed PMID: 27806320. Pubmed Central PMCID: 5347716.
- 687 27. Pan L, Liu Q, Li J, Wu W, Wang X, Zhao D, et al. Association of the VDAC3 gene polymorphism
688 with sperm count in Han-Chinese population with idiopathic male infertility. *Oncotarget*. 2017 Jul
689 11;8(28):45242-8. PubMed PMID: 28431403. Pubmed Central PMCID: 5542182.
- 690 28. Sampson MJ, Lovell RS, Craigen WJ. The murine voltage-dependent anion channel gene family.
691 Conserved structure and function. *The Journal of biological chemistry*. 1997 Jul
692 25;272(30):18966-73. PubMed PMID: 9228078.
- 693 29. Yuan J, Zhang Y, Sheng Y, Fu X, Cheng H, Zhou R. MYBL2 guides autophagy suppressor
694 VDAC2 in the developing ovary to inhibit autophagy through a complex of VDAC2-BECN1-
695 BCL2L1 in mammals. *Autophagy*. 2015;11(7):1081-98. PubMed PMID: 26060891. Pubmed
696 Central PMCID: 4590641.
- 697 30. Xu A, Hua Y, Zhang J, Chen W, Zhao K, Xi W, et al. Abnormal Hypermethylation of the VDAC2
698 Promoter is a Potential Cause of Idiopathic Asthenospermia in Men. *Scientific reports*. 2016 Nov
699 28;6:37836. PubMed PMID: 27892527. Pubmed Central PMCID: 5124954.
- 700 31. Zhu Y, Liu Q, Liao M, Diao L, Wu T, Liao W, et al. Overexpression of lncRNA EPB41L4A-AS1
701 Induces Metabolic Reprogramming in Trophoblast Cells and Placenta Tissue of Miscarriage.
702 *Molecular therapy Nucleic acids*. 2019 Dec 6;18:518-32. PubMed PMID: 31671345. Pubmed
703 Central PMCID: 6838551.

- 704 32. Consortium GT. Human genomics. The Genotype-Tissue Expression (GTEx) pilot analysis:
705 multitissue gene regulation in humans. *Science*. 2015 May 8;348(6235):648-60. PubMed PMID:
706 25954001. Pubmed Central PMCID: 4547484.
- 707 33. Noguchi S, Arakawa T, Fukuda S, Furuno M, Hasegawa A, Hori F, et al. FANTOM5 CAGE
708 profiles of human and mouse samples. *Scientific data*. 2017 Aug 29;4:170112. PubMed PMID:
709 28850106. Pubmed Central PMCID: 5574368.
- 710 34. De Pinto V, Guarino F, Guarnera A, Messina A, Reina S, Tomasello FM, et al. Characterization
711 of human VDAC isoforms: a peculiar function for VDAC3? *Biochimica et biophysica acta*. 2010
712 Jun-Jul;1797(6-7):1268-75. PubMed PMID: 20138821.
- 713 35. Deng W, Roberts SG. A core promoter element downstream of the TATA box that is recognized
714 by TFIIB. *Genes & development*. 2005 Oct 15;19(20):2418-23. PubMed PMID: 16230532.
715 Pubmed Central PMCID: 1257396.
- 716 36. Nepal C, Hadzhiev Y, Balwierz P, Tarifeno-Saldivia E, Cardenas R, Wragg JW, et al. Dual-
717 initiation promoters with intertwined canonical and TCT/TOP transcription start sites diversify
718 transcript processing. *Nature communications*. 2020 Jan 10;11(1):168. PubMed PMID: 31924754.
719 Pubmed Central PMCID: 6954239.
- 720 37. Grandori C, Cowley SM, James LP, Eisenman RN. The Myc/Max/Mad network and the
721 transcriptional control of cell behavior. *Annual review of cell and developmental biology*.
722 2000;16:653-99. PubMed PMID: 11031250.
- 723 38. Thiel G, Cibelli G. Regulation of life and death by the zinc finger transcription factor Egr-1.
724 *Journal of cellular physiology*. 2002 Dec;193(3):287-92. PubMed PMID: 12384981.
- 725 39. Liu ZH, Dai XM, Du B. Hes1: a key role in stemness, metastasis and multidrug resistance. *Cancer*
726 *biology & therapy*. 2015;16(3):353-9. PubMed PMID: 25781910. Pubmed Central PMCID:
727 4622741.
- 728 40. Triner D, Castillo C, Hakim JB, Xue X, Greenson JK, Nunez G, et al. Myc-Associated Zinc Finger
729 Protein Regulates the Proinflammatory Response in Colitis and Colon Cancer via STAT3

- 730 Signaling. *Molecular and cellular biology*. 2018 Nov 15;38(22). PubMed PMID: 30181395.
731 Pubmed Central PMCID: 6206459.
- 732 41. Woo AJ, Kim J, Xu J, Huang H, Cantor AB. Role of ZBP-89 in human globin gene regulation
733 and erythroid differentiation. *Blood*. 2011 Sep 29;118(13):3684-93. PubMed PMID: 21828133.
734 Pubmed Central PMCID: 3186340.
- 735 42. Qu H, Qu D, Chen F, Zhang Z, Liu B, Liu H. ZBTB7 overexpression contributes to malignancy
736 in breast cancer. *Cancer investigation*. 2010 Jul;28(6):672-8. PubMed PMID: 20394500.
- 737 43. Niederreither K, Dolle P. Retinoic acid in development: towards an integrated view. *Nature*
738 *reviews Genetics*. 2008 Jul;9(7):541-53. PubMed PMID: 18542081.
- 739 44. Matson JP, Cook JG. Cell cycle proliferation decisions: the impact of single cell analyses. *The*
740 *FEBS journal*. 2017 Feb;284(3):362-75. PubMed PMID: 27634578. Pubmed Central PMCID:
741 5296213.
- 742 45. Allevato M, Bolotin E, Grossman M, Mane-Padros D, Sladek FM, Martinez E. Sequence-specific
743 DNA binding by MYC/MAX to low-affinity non-E-box motifs. *PloS one*. 2017;12(7):e0180147.
744 PubMed PMID: 28719624. Pubmed Central PMCID: 5515408.
- 745 46. Dong JT, Chen C. Essential role of KLF5 transcription factor in cell proliferation and
746 differentiation and its implications for human diseases. *Cellular and molecular life sciences :*
747 *CMLS*. 2009 Aug;66(16):2691-706. PubMed PMID: 19448973.
- 748 47. Scarpulla RC, Vega RB, Kelly DP. Transcriptional integration of mitochondrial biogenesis.
749 *Trends in endocrinology and metabolism: TEM*. 2012 Sep;23(9):459-66. PubMed PMID:
750 22817841. Pubmed Central PMCID: 3580164.
- 751 48. Hodneland Nilsson LI, Nitschke Pettersen IK, Nikolaisen J, Micklem D, Avsnes Dale H, Vatne
752 Rosland G, et al. A new live-cell reporter strategy to simultaneously monitor mitochondrial
753 biogenesis and morphology. *Scientific reports*. 2015 Nov 24;5:17217. PubMed PMID: 26596249.
754 Pubmed Central PMCID: 4657046.

- 755 49. Costoya JA. Functional analysis of the role of POK transcriptional repressors. Briefings in
756 functional genomics & proteomics. 2007 Mar;6(1):8-18. PubMed PMID: 17384421.
- 757 50. Labrecque MP, Prefontaine GG, Beischlag TV. The aryl hydrocarbon receptor nuclear
758 translocator (ARNT) family of proteins: transcriptional modifiers with multi-functional protein
759 interfaces. Current molecular medicine. 2013 Aug;13(7):1047-65. PubMed PMID: 23116263.
- 760 51. Hayes JD, Dinkova-Kostova AT. The Nrf2 regulatory network provides an interface between
761 redox and intermediary metabolism. Trends in biochemical sciences. 2014 Apr;39(4):199-218.
762 PubMed PMID: 24647116.
- 763 52. Anckar J, Sistonen L. Regulation of HSF1 function in the heat stress response: implications in
764 aging and disease. Annual review of biochemistry. 2011;80:1089-115. PubMed PMID: 21417720.
- 765 53. Morgan R, Pandha HS. PBX3 in Cancer. Cancers. 2020 Feb 13;12(2). PubMed PMID: 32069812.
766 Pubmed Central PMCID: 7072649.
- 767 54. Saghizadeh M, Akhmedov NB, Yamashita CK, Griбанова Y, Theendakara V, Mendoza E, et al.
768 ZBED4, a BED-type zinc-finger protein in the cones of the human retina. Investigative
769 ophthalmology & visual science. 2009 Aug;50(8):3580-8. PubMed PMID: 19369242. Pubmed
770 Central PMCID: 2848067.
- 771 55. Oh S, Hwang ES. The role of protein modifications of T-bet in cytokine production and
772 differentiation of T helper cells. Journal of immunology research. 2014;2014:589672. PubMed
773 PMID: 24901011. Pubmed Central PMCID: 4036734.
- 774 56. Li N, Zhao CT, Wang Y, Yuan XB. The transcription factor Cux1 regulates dendritic morphology
775 of cortical pyramidal neurons. PloS one. 2010 May 11;5(5):e10596. PubMed PMID: 20485671.
776 Pubmed Central PMCID: 2868054.
- 777 57. Hidaka K, Yamamoto I, Arai Y, Mukai T. The MEF-3 motif is required for MEF-2-mediated
778 skeletal muscle-specific induction of the rat aldolase A gene. Molecular and cellular biology. 1993
779 Oct;13(10):6469-78. PubMed PMID: 8413246. Pubmed Central PMCID: 364706.

- 780 58. Kageyama R, Shimojo H, Ohtsuka T. Dynamic control of neural stem cells by bHLH factors.
781 Neuroscience research. 2019 Jan;138:12-8. PubMed PMID: 30227160.
- 782 59. Buratowski S, Zhou H. Functional domains of transcription factor TFIIB. Proceedings of the
783 National Academy of Sciences of the United States of America. 1993 Jun 15;90(12):5633-7.
784 PubMed PMID: 8516312. Pubmed Central PMCID: 46775.
- 785 60. Fang X, Huang Z, Zhou W, Wu Q, Sloan AE, Ouyang G, et al. The zinc finger transcription factor
786 ZFX is required for maintaining the tumorigenic potential of glioblastoma stem cells. Stem cells.
787 2014 Aug;32(8):2033-47. PubMed PMID: 24831540. Pubmed Central PMCID: 4349564.
- 788 61. Basso K, Dalla-Favera R. BCL6: master regulator of the germinal center reaction and key
789 oncogene in B cell lymphomagenesis. Advances in immunology. 2010;105:193-210. PubMed
790 PMID: 20510734.
- 791 62. Bai YQ, Miyake S, Iwai T, Yuasa Y. CDX2, a homeobox transcription factor, upregulates
792 transcription of the p21/WAF1/CIP1 gene. Oncogene. 2003 Sep 11;22(39):7942-9. PubMed
793 PMID: 12970742.
- 794 63. Friedman JR, Kaestner KH. The Foxa family of transcription factors in development and
795 metabolism. Cellular and molecular life sciences : CMLS. 2006 Oct;63(19-20):2317-28. PubMed
796 PMID: 16909212.
- 797 64. Suzuki H, Ahn HW, Chu T, Bowden W, Gassei K, Orwig K, et al. SOHLH1 and SOHLH2
798 coordinate spermatogonial differentiation. Developmental biology. 2012 Jan 15;361(2):301-12.
799 PubMed PMID: 22056784. Pubmed Central PMCID: 3249242.
- 800 65. He S, Yang S, Niu M, Zhong Y, Dan G, Zhang Y, et al. HMG-box transcription factor 1: a positive
801 regulator of the G1/S transition through the Cyclin-CDK-CDKI molecular network in
802 nasopharyngeal carcinoma. Cell death & disease. 2018 Jan 24;9(2):100. PubMed PMID:
803 29367693. Pubmed Central PMCID: 5833394.

- 804 66. Wang W, Lufkin T. Hmx homeobox gene function in inner ear and nervous system cell-type
805 specification and development. *Experimental cell research*. 2005 Jun 10;306(2):373-9. PubMed
806 PMID: 15925593.
- 807 67. Mahnke J, Schumacher V, Ahrens S, Kading N, Feldhoff LM, Huber M, et al. Interferon
808 Regulatory Factor 4 controls TH1 cell effector function and metabolism. *Scientific reports*. 2016
809 Oct 20;6:35521. PubMed PMID: 27762344. Pubmed Central PMCID: 5071867.
- 810 68. Jennings W, Hou M, Perterson D, Missiuna P, Thabane L, Tarnopolsky M, et al. Paraspinal
811 muscle ladybird homeobox 1 (LBX1) in adolescent idiopathic scoliosis: a cross-sectional study.
812 *The spine journal : official journal of the North American Spine Society*. 2019 Dec;19(12):1911-
813 6. PubMed PMID: 31202838.
- 814 69. Musa J, Aynaud MM, Mirabeau O, Delattre O, Grunewald TG. MYBL2 (B-Myb): a central
815 regulator of cell proliferation, cell survival and differentiation involved in tumorigenesis. *Cell*
816 *death & disease*. 2017 Jun 22;8(6):e2895. PubMed PMID: 28640249. Pubmed Central PMCID:
817 5520903.
- 818 70. Zhao M, Mishra L, Deng CX. The role of TGF-beta/SMAD4 signaling in cancer. *International*
819 *journal of biological sciences*. 2018;14(2):111-23. PubMed PMID: 29483830. Pubmed Central
820 PMCID: 5821033.
- 821 71. Moore BD, Jin RU, Lo H, Jung M, Wang H, Battle MA, et al. Transcriptional Regulation of X-
822 Box-binding Protein One (XBP1) by Hepatocyte Nuclear Factor 4alpha (HNF4Alpha) Is Vital to
823 Beta-cell Function. *The Journal of biological chemistry*. 2016 Mar 18;291(12):6146-57. PubMed
824 PMID: 26792861. Pubmed Central PMCID: 4813565.
- 825 72. Wang F, Qiang Y, Zhu L, Jiang Y, Wang Y, Shao X, et al. MicroRNA-7 downregulates the
826 oncogene VDAC1 to influence hepatocellular carcinoma proliferation and metastasis. *Tumour*
827 *biology : the journal of the International Society for Oncodevelopmental Biology and Medicine*.
828 2016 Aug;37(8):10235-46. PubMed PMID: 26831666.

- 829 73. Cam H, Balciunaite E, Blais A, Spektor A, Scarpulla RC, Young R, et al. A common set of gene
830 regulatory networks links metabolism and growth inhibition. *Molecular cell*. 2004 Nov
831 5;16(3):399-411. PubMed PMID: 15525513.
- 832 74. Hughes TR. *A handbook of transcription factors*. Springer Science+Business Media B.V.
833 2011(Subcellular Biochemistry 52).
- 834 75. Guarino FZ, F.; Mela, L.; Pappalardo, X.; Messina, A.; De Pinto, V. NRF-1 and HIF-1 α modulate
835 activity of human VDAC1 gene promoter during starvation and hypoxia in HeLa cells. *Biorxiv*.
836 2020.
- 837 76. Camara AKS, Zhou Y, Wen PC, Tajkhorshid E, Kwok WM. Mitochondrial VDAC1: A Key
838 Gatekeeper as Potential Therapeutic Target. *Frontiers in physiology*. 2017;8:460. PubMed PMID:
839 28713289. Pubmed Central PMCID: 5491678.
- 840 77. Cartharius K, Frech K, Grote K, Klocke B, Haltmeier M, Klingenhoff A, et al. MatInspector and
841 beyond: promoter analysis based on transcription factor binding sites. *Bioinformatics*. 2005 Jul
842 1;21(13):2933-42. PubMed PMID: 15860560.
- 843 78. Fornes O, Castro-Mondragon JA, Khan A, van der Lee R, Zhang X, Richmond PA, et al. JASPAR
844 2020: update of the open-access database of transcription factor binding profiles. *Nucleic acids
845 research*. 2020 Jan 8;48(D1):D87-D92. PubMed PMID: 31701148. Pubmed Central PMCID:
846 7145627.
- 847 79. Gheorghe M, Sandve GK, Khan A, Cheneby J, Ballester B, Mathelier A. A map of direct TF-
848 DNA interactions in the human genome. *Nucleic acids research*. 2019 Feb 28;47(4):e21. PubMed
849 PMID: 30517703. Pubmed Central PMCID: 6393237.
- 850
- 851

Fig. 1 Zinghirino et al

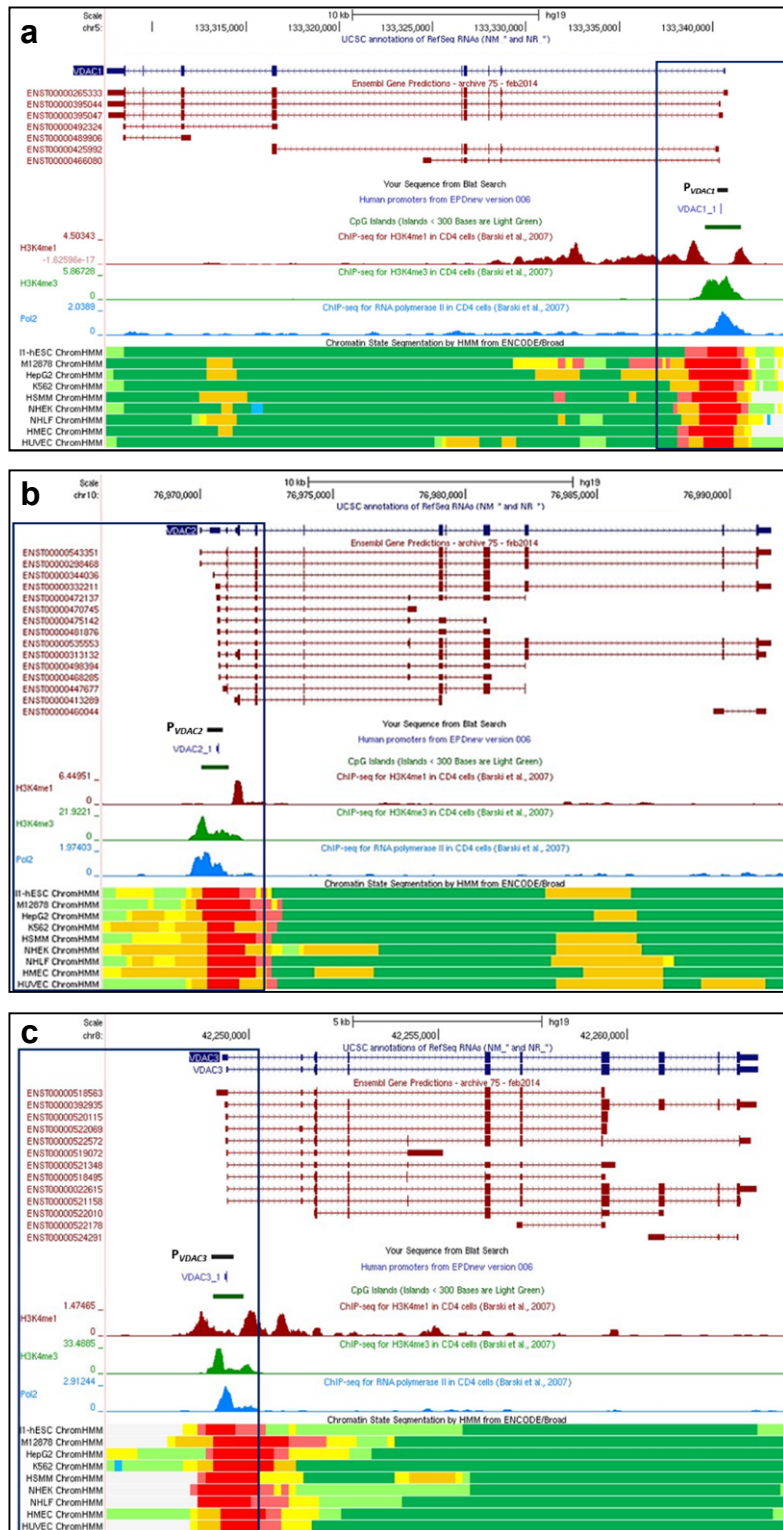
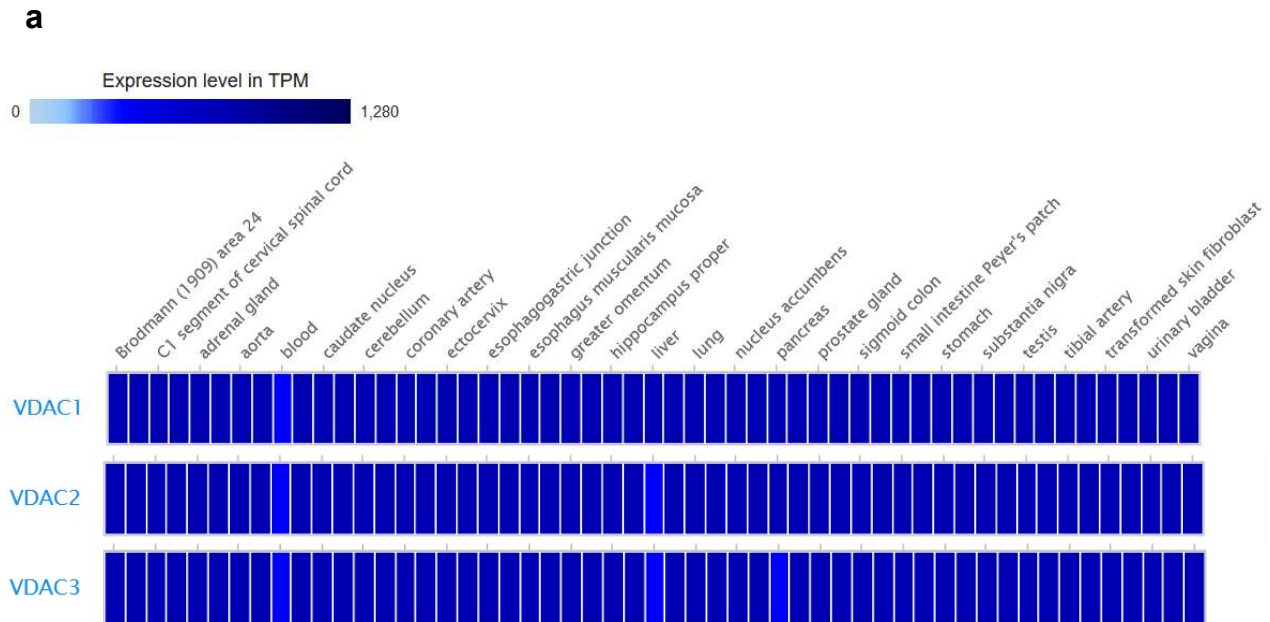


Fig. 2 Zinghirino et al

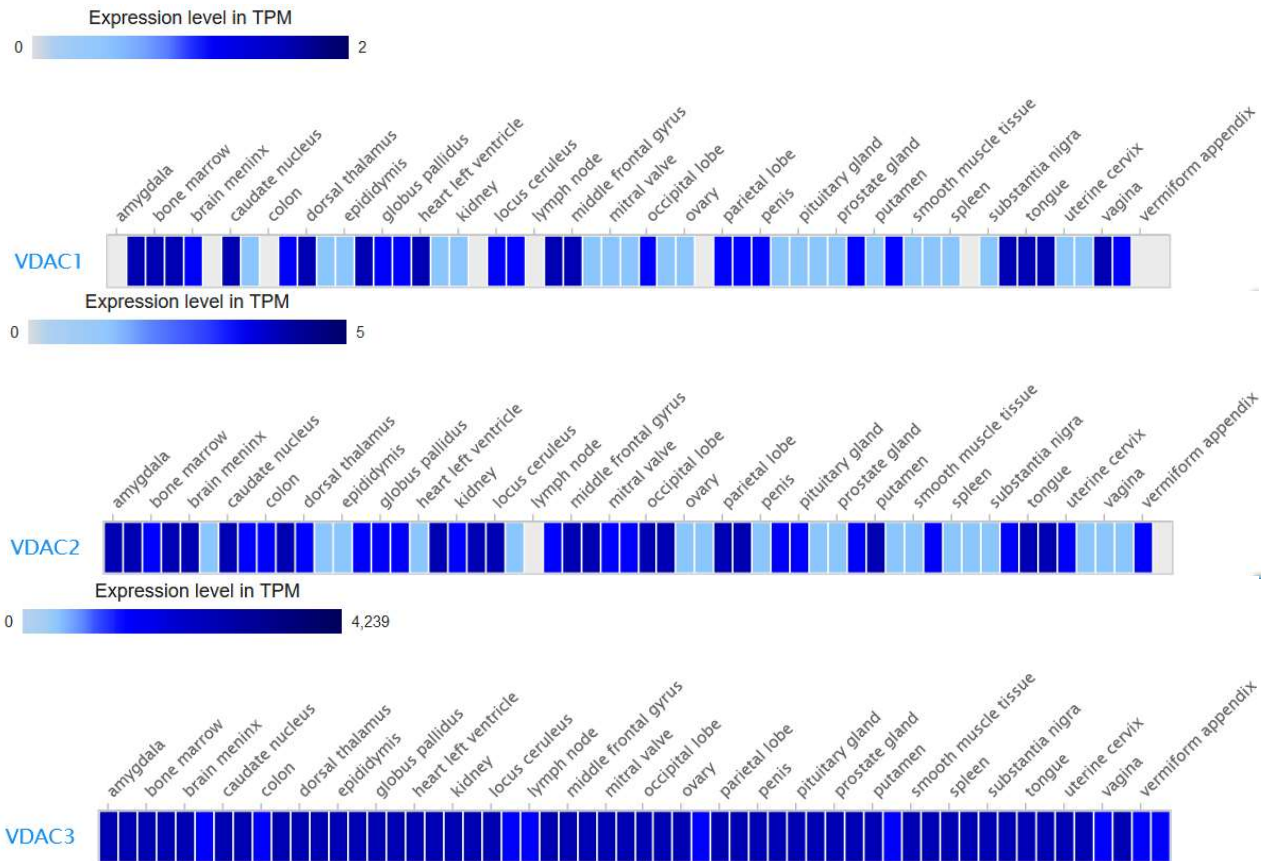


b

VDAC transcripts tissue expression levels RNA-Seq GTEx (TPM values)													
Gene Name	Aorta	Blood	Breast	Cerebral cortex	Heart left ventricle	Liver	Lung	Ovary	Pancreas	Skeletal muscle tissue	Spleen	Stomach	Testis
VDAC1	114.0	23	93	123.0	161.0	84	108	82	49	381	77	133	53
VDAC2	133.0	30	100	69.0	127.0	28	106	131	61	170	72	101	93
VDAC3	81.0	21	57	68.0	81.0	31	66	66	29	139	73	53	103

Fig. 3 Zinghirino et al

a



b

VDAC transcripts tissue expression levels RNA-Seq CAGE-FANTOM 5 project (TPM values)														
Gene Name	Bone marrow	Brain	Breast	Colon	Heart	Kidney	Lung	Lymph node	Ovary	Pancreas	Smooth muscle	Spinal cord	Spleen	Testis
VDAC1	2	1	-	-	0.5	0.2	0.4	-	0.1	-	0.2	0.2	0.3	0.7
VDAC2	0.9	4	0.7	1	1	1	0.8	-	0.8	0.8	0.7	1	0.3	1
VDAC3	66	74	28	38	107	90	30	31	62	35	70	59	58	107

Fig. 4 Zinghirino et al

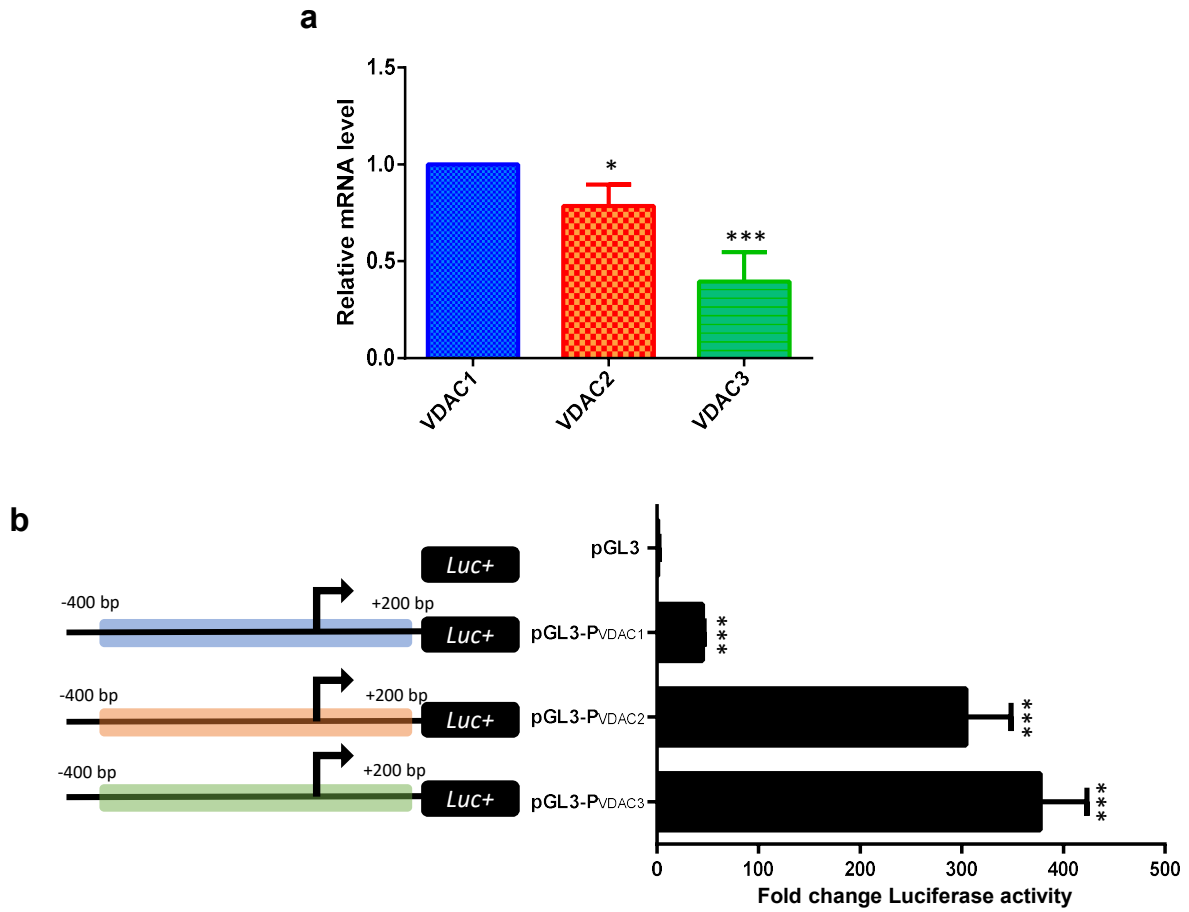


Fig. 5 Zinghirino et al

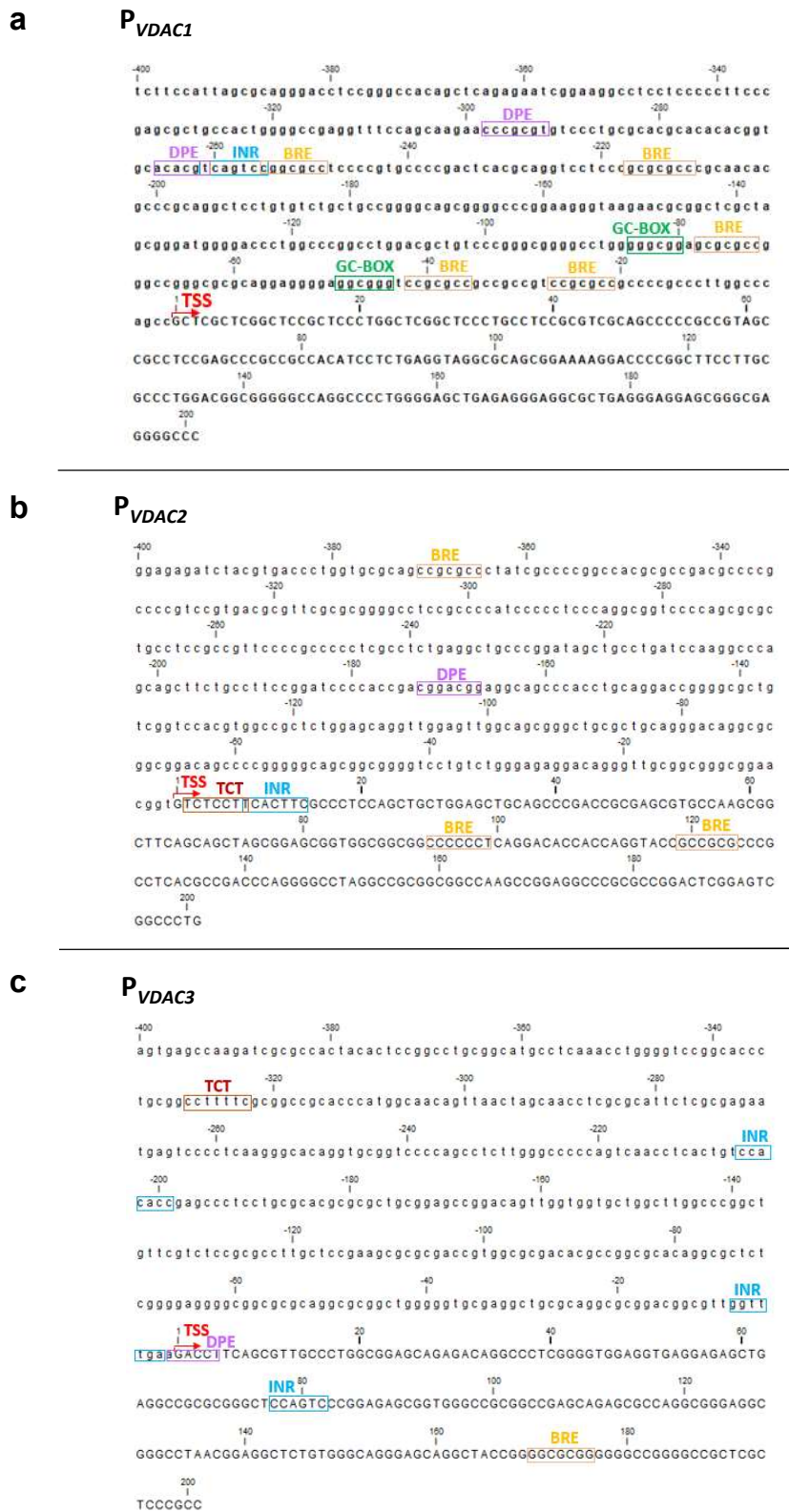


Fig. 6 Zinghirino et al

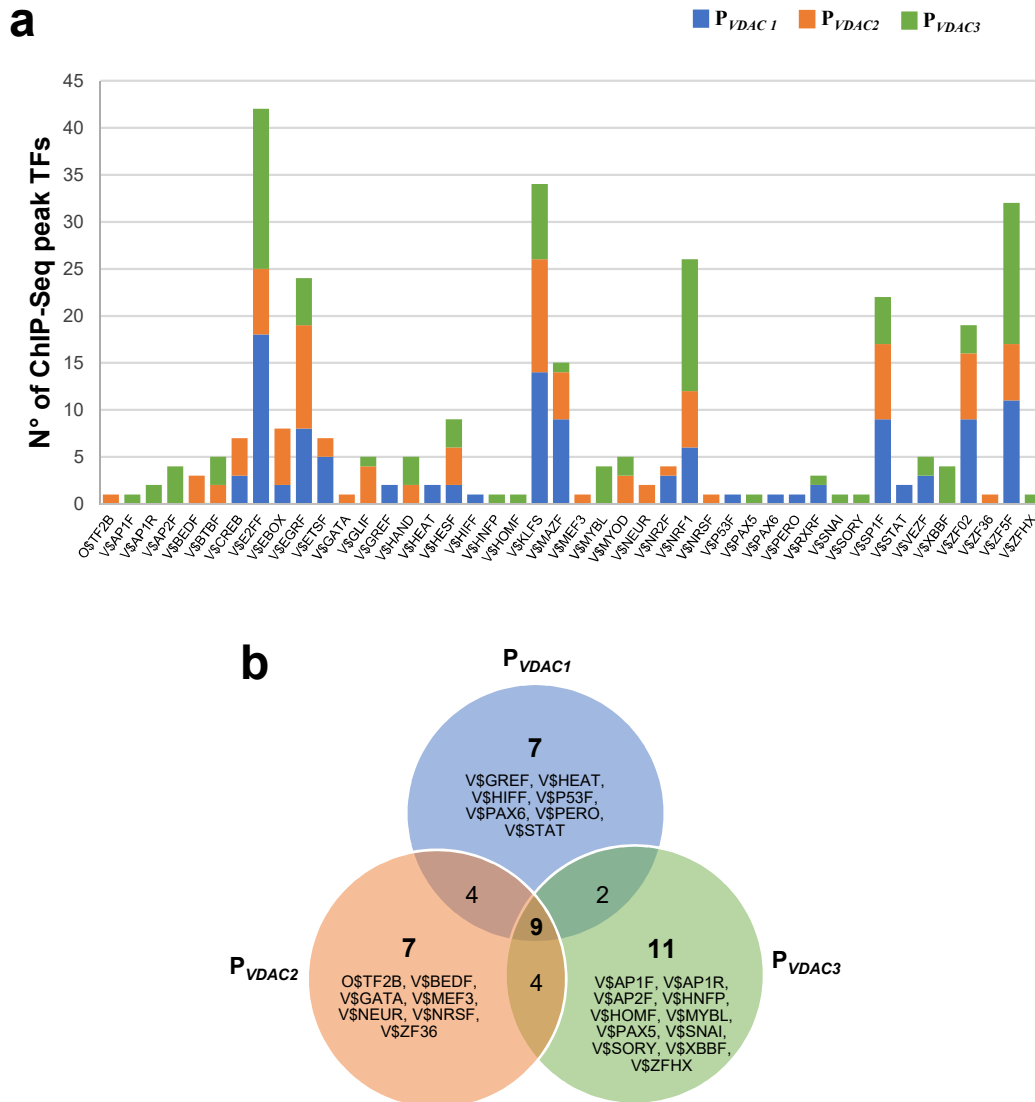


Fig. 7 Zinghirino et al

